

Modelling Local Patterns of Child Mortality Risk. A Bayesian Spatio-Temporal Analysis.

Alejandro Lome-Hurtado (✉ alejandro.lomehu@anahuac.mx)

Universidad Anahuac Mexico <https://orcid.org/0000-0003-1241-4553>

Jacques Lartigue Mendoza

Universidad Anahuac Mexico

Juan Carlos Trujillo

University of York

Research article

Keywords: Children's health, Bayesian mapping, child mortality risk, space-time interactions, Mexico.

Posted Date: November 12th, 2019

DOI: <https://doi.org/10.21203/rs.2.11961/v2>

License:  This work is licensed under a Creative Commons Attribution 4.0 International License.

[Read Full License](#)

Version of Record: A version of this preprint was published at BMC Public Health on January 6th, 2021.

See the published version at <https://doi.org/10.1186/s12889-020-10016-9>.

Abstract

Background : At the international scale the number of child deaths is still high; however, this figure is susceptible to be reduced implementing proper spatially-targeted health public policies. Due to its alarming rate in comparison to North American standards, child mortality is a particular health concern in Mexico. Despite this fact, there remains a dearth of studies that address the spatial-temporal identification of child mortality in Mexico. The aims of this study are i) to model the evolution of child mortality risk at the municipality level in Greater Mexico City, (ii) to identify municipalities with high, medium and low risk over time, and (iii) using municipality trends, to ascertain potential high-risk municipalities. Methods : In order to control for space-time patterns of data, the study performs a Bayesian spatio-temporal analysis. This methodology allows to model the geographical variation of child mortality risk across municipalities within the studied time span. Results : The analysis shows that most of the high-risk municipalities are in the north and west areas of Greater Mexico City, although there coexist some in the east; some of them presenting an increasing child mortality risk trend. The outcomes highlight some municipalities currently presenting a medium risk, but that, given their trend, are likely to become high risk after the studied period. Finally, the likelihood of child mortality risk illustrates an overall decreasing tendency throughout the 7-year studied period. Conclusions : The identification of high-risk municipalities and risk trends may provide a useful input to policy-makers seeking to reduce the incidence of child mortality. The results provide evidence to support geographical targeting for policy interventions.

Introduction

There exists a public concern regarding the high percentage of child mortality. At the international scale, there were 5.6 million child deaths during 2016 [1]. As a consequence, an increasing policy interest in improving children's health has been witnessed, which is reflected in the United Nations' third Sustainable Development Goal (SDG) on good health and wellbeing; particularly, in the SDG 3 target addressed to end preventable deaths of new-born and children under five by the year 2030 [2].

In Mexico, the child mortality rate under 5 years old (per 1,000 live births) decreased from 17.4 in 2010 to 13.4 in 2017. However, these numbers are still higher than those observed in developed countries. For instance, these rates were 7.3 and 6.6 during the referenced years in the United States [3]. Similarly, the probabilities of dying at age 5-14 years (per 1,000 children age 5) in Mexico were 2.8 and 2.5 for the years 2010 and 2018, respectively; while in the United States this figure was 1.3 during the referred years [4]. By the same token, according to the World Bank [5], the Mexican infant mortality rate (per 1,000 live births) observed a reduction from 2011 to 2017, passing from 14.5 to 11.6 respectively. Nevertheless, such rates are still high in comparison to the United States, where the figures were 6.1 and 5.7 during the aforesaid years.

This paper focusses on modelling child mortality risk trends across different geographical areas; contributing, this way, with the international increasing interest in modelling the geographical dimension

of child mortality risk [6]–[9]. Within this research Gayawan et al. [6] illustrated the regional variations of child mortality among 10 West African countries; finding some clusters of higher child mortality in northwest and northeast Nigeria. In the same line, Jimenez-Soto et al. [7] showed the disparities in child mortality across rural-urban locations and regions in Cambodia. Then again, in Papua, New Guinea, a study found important child mortality disparities between rural and urban populations, as well as variations across inter and intra regions [8]. Whereas in Mexico, a similar study [10] analyzed the child mortality trend caused by diarrhoea in all Mexican states; identifying different spatial patterns of the peak mortality rates across time.

The relevance of accounting the potential spatial structure of the data relies on the fact that communities are often clustered with respect to certain shared characteristics, as their socioeconomic background [11]. Hence, it is likely that people with high socioeconomic status live close to each other; which also apply for other socioeconomic standings. However, socioeconomic status should not be the lonely factor underlying child mortality; if the availability of data permits, other variables must be considered under a spatial analysis such as the environment, urbanization, or the genetics of the people [12],[13],[14]. McDonald et al [13], through analysing child mortality in American counties located in the US-Mexico border, found urbanization level as the most relevant variable for explaining child mortality; being the race –hispanic or non-hispanic white– a less relevant variable. Thus, higher mortality rates in non-metropolitan communities were attributed to less access to emergency and special care facilities, limited emergency medical service capabilities, as well as less health care providers per capita. Castro-Ríos et al [14] found that access to social security increases the surviving probability of children with acute lymphoblastic leukemia. More accurately speaking, the research concluded that children who had been insured for less than half their lives had more than double the risk of dying than those who had been insured for their entire lives.

Despite the previous efforts, there still exists a need for analyzing not just the spatial pattern but also the local trend over time of such mortality risk, at the geographical level, in order to gain a better understanding. In this sense, socioeconomic status may also vary across time, for individuals and/or neighbourhoods, with a relevant influence on health risk [11]. Consequently, child mortality may not only vary over space, but also over time, as it has been concluded from previous health studies; such is the case of the spatio-temporal variations of stomach cancer risk [15] and asthma risk [16]. Besides, people's health risk may vary over space and time due to different factors, among them changes in health-related behaviours, such as physical activity, smoking, and diet [17].

The aims of this study are (i) to model the evolution of child mortality risk at the municipality level in Greater Mexico City, (ii) to identify municipalities with high, medium and low risk over time, and (iii) using local trends, to ascertain potential high-risk municipalities. Note that in this study, due to the limitations of the data in the Mexican context, we defined child mortality risk as the ratio of child deaths divided by total dead people.

Regarding health policies, locations with high child mortality risk should be benefited from priority interventions. In this sense, this analysis provides important baseline information for decision-makers. In the same line, the identification of spatial and temporal trends across different areas provides important inputs for decision-makers in designing programmes to tackle health inequalities [18]. Using these inputs, spatially targeted programmes may focus on small locations, allowing policy measures to have a more effective local impact. In this regard, it has already been demonstrated that in comparison with other programmes, where the resources are not addressed towards specific geographical areas [19], [20], vulnerable and local groups are more benefited when the aforementioned inputs are used.

This study uses a Bayesian modelling approach [21] due to the space, time, and space-time structure of the data, the methodology is based on random effects, which permits to model the geographical variation of children mortality over time. It must be acknowledged that the methodology applied in this study has been used in the area of criminology [22].

Data And Methods

2.1 Area of study and Children mortality data

Greater Mexico City, one the most populated urban areas in the world, is the third largest metropolis in OECD countries, and the world's largest outside Asia [23]. It consists of 16 municipalities within Mexico City and 59 municipalities of the State of Mexico (see figure A2 in the Appendix). It had 20,892,724 inhabitants in 2015, According to the Mexican National Institute of Statistics and Geography (INEGI) [24], it had 20,892,724 inhabitants in 2015, coveringwith a land area of 7,866 square kilometers. In economic terms, ilt is considered the most important metropolitan area in Mexico, in terms of the economy, producing 23% of the country's gross domestic product in 2010 [23]. The study explored the catalog of death records of the Mexican Ministry of Healththe, catalog of death records of the Mexican Ministry of Health forin the municipalities of Greater Mexico City; covering 75 municipalities, from January 2011 to December 2017. During the study period, tThe total number of deathth records in the region wasere n = 789,44015 and among them there were 39,263 dead children in the region, in the study period. This information was aggregated in order to perform a spatial and temporal analysis, at the municipality level [25]. Children were considered from 0 to 12 years old [26].

In order to analyze the potential presence of spatial autocorrelation and serial correlation of these data, the Global Moran Index [27] and the Autocorrelation Function (ACF) statistical tests were carried out in order to analyze the potential presence of spatial autocorrelation and serial correlation of the data, respectively. The Global Moran Index of the data for each year was positive and significant, with a mean value of 0.32 and a p value < 0.0001 , this illustratinges the presence of positive spatial autocorrelation in the records. In other words, tThis result is indicative of showed the existence of some nearby municipalities with similar mortality risk. The ACF mean was 0.58 (lagged 1 year for each municipality), across all the municipalities. This number illustrated the evidences the presence of serial correlation; that is,, the association ofn a certain level of the observed mortality data across time.

2.2 Statistical analysis

To model the potential spatial, temporal and spatio-temporal structure of the child mortality data, the current study performed a Bayesian analysis. For modelling the probability of having a child death or not, the death analysis assumes a binomial distribution [28], $y_{it} \sim \text{Binomial}(n_{it}, \mu_{it})$. Specifically, let y_{it} be the number of cases of dead children in each municipality i at the time period t ($= 2011, 2012, 2013, \dots, 2017$); n_{it} represents the number of total of dead children people in the municipality i at the time period t ; and μ_{it} denotes children mortality risk the child mortality risk in the municipality i at the time period t . According to Law et al. [29] and Li et al. [22] the child mortality risk can be modelled as:

$$\text{logit}\mu_{it} = a + s_i + u_i + d_0 t^* + v_t + d_1 i t^* + \varepsilon_{it} \quad (1)$$

where a is the overall logit child mortality risk across the 76-year period; while the terms s_i and u_i capture the spatial structure of the data. These components are common over the study period. In turn, $d_0 t^* + v_t$ are the overall time trend to all the municipalities. The first term ($d_0 t^*$) assesses the linear trend and the second, v_t , with additional Gaussian noise, allows for nonlinearity in the overall trend pattern; v_t has the distribution $v_t \sim N(0, \sigma_v^2)$. Note that t^* is centered at the mid observation period, $t^* = t - 4$. The following expression, $d_1 i t^*$, denotes the spatial-temporal structure of the data which allows each municipality to have different trends from the overall time trend-pattern. This term plays an important role due to child mortality trends exhibit variability at the local level (see figure 1). $d_1 i t^*$ represents and assumes a linear departure of the local temporal trend of each municipality from the common trend; such local trend can have an increasing, decreasing or a stable tendency from the overall linear pattern. Finally, $\varepsilon_{it} \sim N(0, \sigma_\varepsilon^2)$ is the component for the variability that is not explained by the other terms. This may include overdispersion, that is, when the variation of the data is higher than its mean. Overdispersion is common in binomial models [30], [31].

We assigned the BYM (Besag, York and Mollié) model [32] to the spatial components. Following previous studies [18], [19], [25] we allocated an intrinsic conditional autoregressive Gaussian distribution (ICAR) to the priors for the spatial structure (s_i) and the spatio-temporal interaction terms (d_i). Thus, the term d_i , and similarly for s_i , depends on the neighbouring; it means that neighbouring areas are more likely to have similar values. In our specific case, it means that nearby municipalities are assumed to have similar child mortality risk rates. This is controlled by a spatial adjacency matrix W of size $N \times N$, where the diagonal values are $w_{ii} = 0$ and the off-diagonal entries $w_{ij} = 1$ if municipalities i and j share a common boundary, otherwise $w_{ij} = 0$. In this sense, if two municipalities are defined to be neighbours their random effects are correlated, otherwise they are conditionally independent. The conditional expectation of d_i is equal to the mean of the random effects in neighbouring municipalities, whereas the conditional variance is inversely proportional to the number of neighbour municipalities, this similarly for s_i . Note that d_i may also control for the potential endogeneity due to the interaction between space and time. As previous studies [19], [25] we allocated an hyperprior distribution of Gamma, a highly non-informative distribution [33], on the variance of d_i and similarly to the variance for s_i . We assigned a Gaussian distribution to the

spatially unstructured random effect term, u_i . Finally, all random effect standard deviations, such as σ^2 and σ_e , have a positive half Gaussian prior $N^{+\infty}(0,10)$ following the Gelman criterion [34].

To classify each municipality into hot, cold or neither-hot-nor-cold spots (high, low or medium risk) across time, we used the values of the posterior probability of the spatial component $p_{expui+si > 1}$. The component $p_{expui+si}$ indicates the odds average risk of the study period for each municipality with respect to a (overall logit children mortality risk). Thus, the values greater than 0.8, between 0.2 and 0.8, and lower than 0.2 were classified as hot, neither-hot-nor-cold spots and cold spots (high, low and medium risk municipalities), respectively. This first classification can be expressed in the hi term which is equal to 1 for a hotspot, equal to 2 for a cold spot, and equal to 3 for a neither-hot-nor-cold spot. This criterion has been used in previous studies [22], [35]. Next, to measure the local trend of each classified municipality, we used the values of the posterior probability of the local slopes d_{1i} given a specific category of hi . This allowed to measure the local dynamic pattern of each municipality over the study period. Thus, if $p_{d_{1i} > 0 | hi, data} > 0.8$, $p_{d_{1i} > 0 | hi, data} < 0.2$ or $0.2 < p_{d_{1i} > 0 | hi, data} < 0.8$ the municipality was classified with an increasing, decreasing or stable trend in comparison with the overall trend.

The model was implemented in R and WinBUGS (statistical software). We ran MCMC chains of 100,000 (for this number the model reaches convergence) with different initial values for the model. 70,000 iterations were used for making inferences from the model, after having burned in the first 30,000. The convergence was examined by visual inspection of the history plots and through the Gelman-Rubin diagnostic [34], which are standard statistical tests to measure convergence of MCMC chains. The values from the Gelman-Rubin diagnostic remained lower than 1.04 for every single model parameter, showing that the chains achieved convergence after the burn-in period.

Results

3.1 Descriptive Analysis

The Global Moran Index of the data for each year was positive and significant, with a mean value of 0.32 and a p value < 0.0001 , illustrating the presence of positive spatial autocorrelation in the records. In other words, this result is indicative of the existence of some nearby municipalities with similar mortality risk. The ACF mean was 0.58 (lagged 1 year for each municipality) across all the municipalities. This number evidences the presence of serial correlation; that is, the association of certain level of observed mortality across time.

Table 1 provides a descriptive statistics overview of the observed child mortality risk –(child deaths / total deaths) $\times 100$ – in Greater Mexico City. Overall, a slight mitigation on the average child mortality risk during these years (8.17, 6.54, and 5.41 during 2011, 2014 and 2017, respectively) was observed. Note that according to the means and variances, illustrated in table 1, there was a trace of overdispersion in our data.

Figure 1 illustrates the temporal evolution of the observed child mortality risk by municipality in Greater Mexico City, at different time points –2011, 2014, and 2017 (start, middle, and end)– throughout the study period. The green and red colours show the lower and higher risks, respectively. Overall, municipalities with higher risk were in the north, east, and partially in the west. Conversely, there was a clear cluster (stronger green colour) located in the centre-west which had the lowest mortality risk.

3.2 Modelling spatial-temporal patterns

Figure 2a illustrates the likelihood of child mortality risk by municipality, compared with respect to the average over the studied period. Thus, a probability risk value that is above or below 1 suggests a higher or lower risk, for the respective municipality, in comparison to the Greater Mexico City 7-year average. The figures mostly show that the municipalities belonging to the north and west areas, as well as a few in the east –in general the surroundings municipalities of Greater Mexico City–, were characterized by having higher risks of children mortality. Whilst, broadly speaking, Mexico City's municipalities, as well as a few of them in the north of the studied area, presented lower risks of child mortality. Figure 2b illustrates the overall time trend of relative risk, compared to Greater Mexico City average from 2011 to 2017. Overall, as can be observed, there was a slight decreasing tendency of such risk.

Figure 3a, 3b, and 3c show the hot spots, neither-hot-nor-cold spots, and cold spots of child mortality risk by municipality (high, medium, and low risk, respectively). There were 39 (52.0% of the total), 16 (21.3% of the total) and 20 (26.6% of the total) municipalities with high, medium, and low risk, respectively. In general, high risk municipalities were located in the north, west and east of the metropolitan area with a few spots in the south (see Figure 3a). Meanwhile, most of the low risk municipalities were located in the center (Mexico City) and its surrounding municipalities in the north-west area (figure 3b). Finally, figure 3c shows that the medium risk municipalities were mostly scattered in the north and south-west. All these classified municipalities were significant at the 95% Credible Interval (CI).

The inserted small graphs in figures 3a, 3b, and 3c show the different trends of the observed risk (black solid dots), the estimated risk (dashed line with open circles) with 95% CI (grey region), and the estimated common trend (black line) of the mortality risk over time.

Figure 3a shows that most of the high-risk municipalities (72%) had a stable dynamic, whereas 6 of the high-risk municipalities (representing 15%) had an increasing trend in children mortality risk. Leaving just 5 high-risk municipalities (13%) with a decreasing trend over time. Figure 3b shows the medium risk municipalities, of which 25% presented an increasing trend in risk. The majority of these medium risk municipalities presented a stable tendency (50%); whereas, those municipalities with a decreasing trend represented the 25%.

Finally, Figure 3c illustrates that a few number of low risk municipalities, 15%, mainly located in Mexico City downtown, experienced a relative increment in child mortality risk over time. However, most of these low risk municipalities (65%) had a stable trend during the studied period; leaving just 20% of municipalities, under this category, with a decreasing trend.

Discussion

This research studied the children mortality dynamics, across municipalities, in Greater Mexico City. It identified those municipalities with high child mortality risk, as well as those with medium risk that, given their trend, may become high risk.

Our findings illustrate that around 50% of the high-risk municipalities are in the north, west and east of Greater Mexico City, with a few spots in the south. This is an expected result since the best economic and socioeconomic conditions are located in the center, that is, in Mexico City; being the surrounding municipalities those with lower economic and social standings. According to INEGI, the north, west and east areas of Greater Mexico City are characterized by having relatively lower socioeconomic and education levels than the average (see figure A2 in the Appendix). The previous results are in line with Sreeramareddy C. et al [36], and Aheto J. [37], which state there exists a positive association between deprived economic conditions and child mortality; meaning that the lower the level of income, the higher the probabilities of having larger child mortality rates.

In terms of risk evolution, six high-risk municipalities (Nextlalpan, Ozumba, Tenango del Aire, Tequixquiac, Tultepec and Tonanitla) presented an increasing trend over time, most of them located in the north area. Similarly, there were 4 medium risk municipalities (Apaxco, Chiconcuac, Teotihuacán and Tlalmanalco), representing 25% of the total medium risk municipalities, with an increasing trend over time; meaning that they may become high risk in the short term. With the exception of Tlalmanalco, which also faces deprived economic and social conditions, the previous municipalities are located in the north of Greater Mexico City (see figure A1 in the Appendix). The previous results are congruent with those of Escamilla-Santiago et al [38], who found, for the period 1990 - 2009, an increasing cancer mortality rate in children and teenagers belonging to high marginalized Mexican states.

It must be acknowledged that the average mortality risk likelihood presents a decreasing trend over the 7-years studied period. This result is congruent with that of Aguirre A. and Vela-Péón F. [39] who estimated, by deploying the Brass mortality method, a decreasing infant mortality rate in Mexico from 1990 to 2010. This slight decrement may partially be explained as the result of different public health policies. For instance, the Ministry of Health in Mexico has created a number of public programmes to decrease the neonatal mortality risk. These include "Programa de Acción: Arranque Parejo en la Vida, 2002",

"Programa de Acción Específico 2007-2012, 2008" and "Programa de Acción Específico Salud Maternal y Perinatal, 2013-2018" [40].

Finally, it is missing to mention that, due to some data limitations, the results here exposed require a word of caution. Specifically, we assumed there is not mobility of children. Although this assumption may not apply in a dynamic area, as Greater Mexico City, more precise unavailable data would be required for considering this factor. Thus, as a consequence, the mobility of people was not included as in other studies [41], [42]. Despite the previous constraint, we hope the key strengths of this study, including space, time, and space-time structures, may provide relevant insights for diminishing child mortality risk in Greater Mexico City. In this sense, McLaughlin et al. [43] highlight the importance of spatial data, and the local context, as inputs for policy decisions. While in the area of health, Ugarte et al. [36] illustrate that spatial and temporal trends provide useful information for addressing health inequalities. However, in order to complement this study, future studies should be targeted to investigate additional potential factors underlying child mortality risk.

Conclusion

By unearthing the identification and evolution of child mortality risk on those municipalities belonging to Greater Mexico City, the findings of this research may provide an important input for policy decisions addressed to reduce the mortality of children. In this sense, the identification of municipalities with medium and high child mortality risk, especially those with an increasing trend over time (Nextlalpan Ozumba, Tenango del Aire, Tequixquiac, Tultepec, and Tonanitla, in the case of high child mortality risk), would permit the geographical targeting of policy efforts to reduce it. Given the overall scarcity of healthcare resources in Mexico, we hope the results may contribute to the improvement of cost-effective policies.

Declarations

Acknowledgements

We are grateful with Li Guanquan for the meetings which favoured the proper understanding of the Bayesian model; as well as with Paloma Botello and Mekuria Asfaw for their enlightening comments / feedback that helped to the improvement of this paper.

Ethics approval and consent to participate

Not applicable

Consent for publication

Not applicable

Availability of data and material

Data are freely available at:

http://www.dgis.salud.gob.mx/contenidos/basesdedatos/Datos_Abiertos_gobmx.html

Competing interests

The authors declare that they have no competing interests.

Funding

No funding required

Authors' contributions

ALH developed the spatio-temporal statistical model and performed the model programming, fitting and interpretation of the results. He drafted the sections in this paper.

All the authors contributed to the design of the study.

JCT and JLM contributed with the introduction, discussion and conclusions. They wrote the final manuscript.

All authors read and approved the final manuscript.

Author details

1 Anahuac University, Mexico.

2 University of York, England.

References

- [1] You, D. *et al.*, "United Nations Inter-agency Group for Child Mortality Estimation (UN IGME). Global, regional, and national levels and trends in under-5 mortality between 1990 and 2015, with scenario-based projections to 2030: a systematic analysis by the UN Inter-agency , " *Lancet*, vol. 386, no. 10010, pp. 2275–2286, 2015.
- [2] Nations, U., "Sustainable development goals," (*n.d.*). [Online]. Available: <https://www.un.org/sustainabledevelopment/health>.
- [3] Bank, T. W., "Mortality rate, under-5 (per 1,000 live births)," (*n.d.*). [Online]. Available: <https://data.worldbank.org/indicator/SH.DYN.MORT?end=2017&locations=MX&start=1960&view=chart>.
- [4] Hill, K., L. Zimmerman, and D. T. Jamison, "Mortality risks in children aged 5-14 years in low-income and middle-income countries: A systematic empirical analysis," *Lancet Glob. Heal.*, vol. 3, no. 10, pp. e609–e616, 2015.

- [5] Bank, T. W., "Mortality rate, infant (per 1,000 live births)," (n.d). [Online]. Available: <https://data.worldbank.org/indicator/SP.DYN.IMRT.IN?view=chart>.
- [6] Gayawan, E., M. I. Adarabioyo, D. M. Okewole, S. G. Fashoto, and J. C. Ukaegbu, "Geographical variations in infant and child mortality in West Africa: A geo-additive discrete-time survival modelling," *Genus*, vol. 72, no. 1, 2016.
- [7] Jimenez-soto, E., J. Durham, and A. Hodge, "Entrenched Geographical and Socioeconomic Disparities in Child Mortality: Trends in Absolute and Relative Inequalities in Cambodia," vol. 9, no. 10, 2014.
- [8] Bauze, A. E. *et al.*, "Equity and Geography: The Case of Child Mortality in Papua New Guinea," vol. 7, no. 5, 2015.
- [9] Singh, A., P. K. Pathak, R. K. Chauhan, and W. Pan, "Infant and Child Mortality in India in the Last Two Decades: A Geospatial Analysis," vol. 6, no. 11, 2011.
- [10] Alonso, A. W. J. *et al.*, "Spatio-temporal patterns of diarrhoeal mortality in Mexico Stable URL: <https://www.jstor.org/stable/41408329> REFERENCES Linked references are available on JSTOR for this article: Spatio-temporal patterns of diarrhoeal mortality in Mexico," vol. 140, no. 1, pp. 91–99, 2019.
- [11] Knorr-Held, L. and J. Besag, "Modelling risk from a disease in time and space," *Stat. Med.*, vol. 17, no. 18, pp. 2045–2060, 1998.
- [12] Lome-Hurtado, A., J. Touza-Montero, and P. C. L. White, "Environmental Injustice in Mexico City: A Spatial Quantile Approach," *Expo. Heal.*, pp. 1–15, 2019.
- [13] McDonald, J. A., L. Brantley, and L. J. Paulozzi, "Mortality , Ethnicity , and Urbanization Among Children Aged 1-4 Years on the US-Mexico Border," vol. 133, no. 5, pp. 593–600, 2018.
- [14] Castro-Ríos, A., H. Reyes-Morales, B. E. Pelcastre-Villafuerte, M. E. Rendón-Macías, and A. Fajardo-Gutiérrez, "Socioeconomic inequalities in survival of children with acute lymphoblastic leukemia insured by social security in Mexico: a study of the 2007–2009 cohorts," *Int. J. Equity Health*, vol. 18, no. 1, p. 40, 2019.
- [15] Papoila, A. L. *et al.*, "Stomach cancer incidence in Southern Portugal 1998–2006: A spatio-temporal analysis," *Biometrical J.*, vol. 56, no. 3, pp. 403–415, 2014.
- [16] Lawson, A. B., *Bayesian disease mapping: hierarchical modeling in spatial epidemiology*. Chapman and Hall/CRC, 2013.
- [17] Shin, H. H., D. Stieb, R. Burnett, G. Takahara, and B. Jessiman, "Tracking National and Regional Spatial-Temporal Mortality Risk Associated with NO₂ Concentrations in Canada: A Bayesian Hierarchical Two-Level Model," *Risk Anal. An Int. J.*, vol. 32, no. 3, pp. 513–530, 2012.

- [18] Ugarte, M. D., A. Adin, T. Goicoa, I. Casado, E. Ardanaz, and N. Larrañaga, "Temporal evolution of brain cancer incidence in the municipalities of Navarre and the Basque Country, Spain," *BMC Public Health*, vol. 15, no. 1, pp. 1–7, 2015.
- [19] Smith, G., "Area-based initiatives: the rationale and options for area targeting," *LSE STICERD Res. Pap. No. Case025*, 1999.
- [20] Tunstall, R. and R. Lupton, "Is Targeting Deprived Areas an Effective Means to Reach Poor People? An assessment of one rationale for area-based funding programmes," 2003.
- [21] Bernardinelli, L., D. Clayton, C. Pascutto, C. Montomoli, M. Ghislandi, and M. Songini, "Bayesian analysis of space–time variation in disease risk," *Stat. Med.*, vol. 14, no. 21-22, pp. 2433–2443, 1995.
- [22] Li, G., R. Haining, S. Richardson, and N. Best, "Space-time variability in burglary risk: A Bayesian spatio-temporal modelling approach," *Spat. Stat.*, vol. 9, no. C, pp. 180–191, 2014.
- [23] (OECD), O. for E. C. and D., "Territorial Reviews: Valle de México, Mexico," 2015. [Online]. Available: http://www.keepeek.com/Digital Asset-Management/oecd/urban-rural-and-regional-development/oecd-territorial-reviews-valle-de-mexico-mexico/urban-trends-and-challenges-of-the-valle-de-mexico_9789264245174-5-en.
- [24] (INEGI), M. N. I. of S. and G., "Población," (n.d.). [Online]. Available: <https://www.inegi.org.mx/temas/estructura/>.
- [25] Lome-Hurtado, A., "Child mortality data set in Greater Mexico City," *Mendeley Data*, vol. 1, 2019.
- [26] Administration, U. F. and D., "General clinical pharmacology considerations for pediatric studies for drugs and biological products. Clinical Pharmacology," 2014. [Online]. Available: <https://www.fda.gov/Drugs/GuidanceComplianceRegulatoryInformation/Guidances/default.htm>.
- [27] Anselin, L., A. K. Bera, R. Florax, and M. J. Yoon, "Simple diagnostic tests for spatial dependence," *Reg. Sci. Urban Econ.*, vol. 26, no. 1, pp. 77–104, 1996.
- [28] McCullagh, P., *Generalized linear models*. Routledge, 2019.
- [29] Law, J., M. Quick, and P. Chan, "Bayesian spatio-temporal modeling for analysing local patterns of crime over time at the small-area level," *J. Quant. Criminol.*, vol. 30, no. 1, pp. 57–78, 2014.
- [30] Dean, C. B., "Testing for overdispersion in Poisson and binomial regression models," *J. Am. Stat. Assoc.*, vol. 87, no. 418, pp. 451–457, 1992.
- [31] Yang, Z., J. W. Hardin, and C. L. Addy, "A note on Dean's overdispersion test," *J. Stat. Plan. Inference*, vol. 139, no. 10, pp. 3675–3678, 2009.

- [32] Besag, J., J. York, and A. Mollié, "A Bayesian image restoration with two applications in spatial statistics Ann Inst Statist Math 43: 1–59," *Find this Article online*, vol. 43, no. 1, pp. 1–20, 1991.
- [33] Kelsall, J. E. and J. C. Wakefield, "Discussion of 'Bayesian models for spatially correlated disease and exposure data', by Best et al," *Bayesian Stat.*, vol. 6, p. 151, 1999.
- [34] Gelman, A. and D. B. Rubin, "Inference from iterative simulation using multiple sequences," *Stat. Sci.*, vol. 7, no. 4, pp. 457–472, 1992.
- [35] Richardson, S., A. Thomson, N. Best, and P. Elliott, "Interpreting posterior relative risk estimates in disease-mapping studies," *Environ. Health Perspect.*, vol. 112, no. 9, pp. 1016–1025, 2004.
- [36] Sreeramareddy, C. T., H. N. Harsha Kumar, and B. Sathian, "Time trends and inequalities of under-five mortality in Nepal: A secondary data analysis of four demographic and health surveys between 1996 and 2011," *PLoS One*, vol. 8, no. 11, pp. 1–12, 2013.
- [37] Aheto, J. M. K., "Predictive model and determinants of under-five child mortality: Evidence from the 2014 Ghana demographic and health survey," *BMC Public Health*, vol. 19, no. 1, pp. 1–10, 2019.
- [38] Escamilla-santiago, R. A. *et al.*, "Tendencia de la mortalidad por cáncer en niños y adolescentes según grado de marginación en México (1990-2009)," vol. 54, no. 6, pp. 587–594, 2012.
- [39] Aguirre, A. and F. Vela-pe, "La mortalidad infantil en México, 2010," pp. 1–15, 2010.
- [40] Mexico, M. of H. in, "Programa de Accion Especifico. Salud Maternal y Perinatal," 2014. [Online]. Available: <https://www.gob.mx/cms/uploads/attachment/file/242370>.
- [41] Havard, S., S. Deguen, D. Zmirou-Navier, C. Schillinger, and D. Bard, "Traffic-related air pollution and socioeconomic status: a spatial autocorrelation study to assess environmental equity on a small-area scale," *Epidemiology*, pp. 223–230, 2009.
- [42] Fecht, D. *et al.*, "Associations between air pollution and socioeconomic characteristics, ethnicity and age profile of neighbourhoods in England and the Netherlands," *Environ. Pollut.*, vol. 198, pp. 201–210, 2015.
- [43] McLaughlin, L. M., S. D. Johnson, K. J. Bowers, D. J. Birks, and K. Pease, "Police perceptions of the long-and short-term spatial distribution of residential burglary," *Int. J. Police Sci. Manag.*, vol. 9, no. 2, pp. 99–111, 2007.

Table 1

Table 1. Descriptive statistics. Observed child mortality risk¹ in Greater Mexico City (2011 to 2017)

Observed child mortality risk	2011 year	2012 year	2013 year	2014 year	2015 year	2016 year	2017 year
Mean	8.17	7.73	6.85	6.54	6.15	5.21	5.41
Standard deviation	3.15	3.03	2.52	3.08	2.58	2.16	2.23
Minimum value ²	1.58	1.41	0.00	1.63	1.49	1.30	1.33
Maximum value ³	17.65	15.79	12.28	15.79	14.55	13.21	10.37

1/ Child mortality risk = (child deaths / total deaths) x 100.

2/ Corresponds to the municipality with the minimum value among all the municipalities of Greater Mexico City.

3/ Corresponds to the municipality with the maximum value among all the municipalities of Greater Mexico City.

Figures

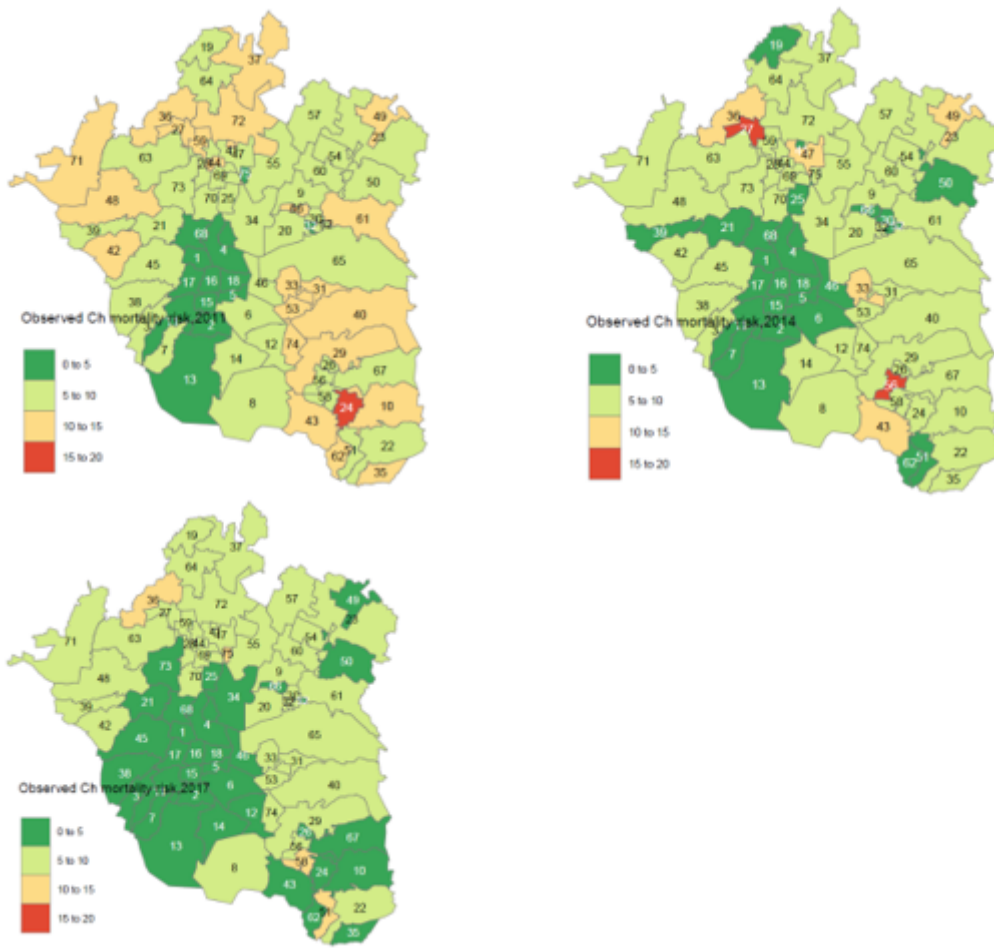


Figure 1

Temporal evolution of the geographical pattern of the observed child mortality risk (per 100) in Greater Mexico City. Figure 1 show the temporal evolution of the geographical pattern of the observed child

mortality risk (per 100) in Greater Mexico City, at the start, middle, and end (2011, 2014, and 2017) of the studied period.

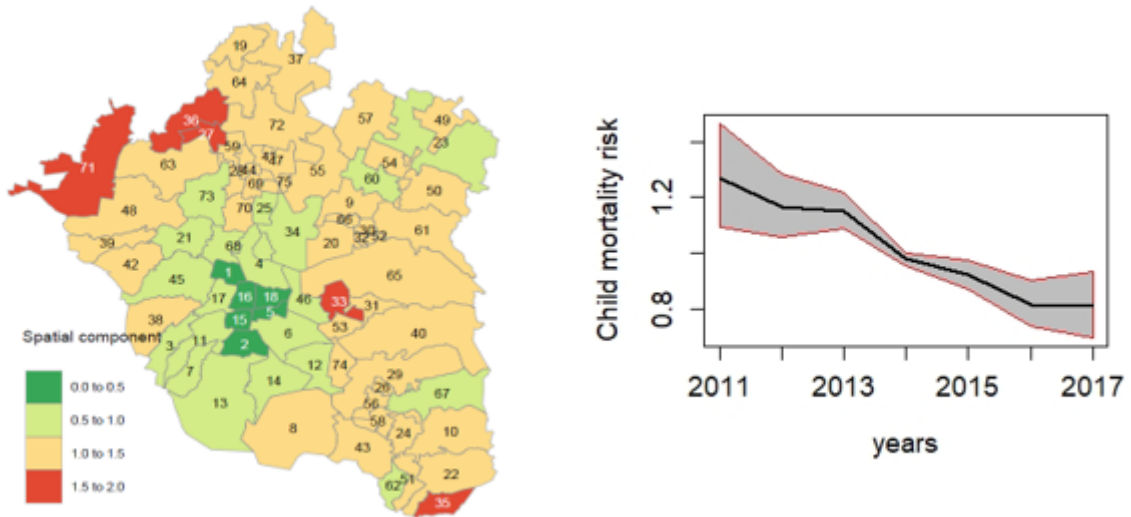


Figure 2

Spatial child mortality risk at the municipality level and overall trend in Greater Mexico City. Figure 2a. shows the spatial component of child mortality odd risk during the studied period. Those areas with odd risk values greater or lower than 1 have higher or lower odd risks in comparison with the average, respectively. Figure 2b displays the overall odd risk trend, with a 95% CI, from 2011 to 2017.

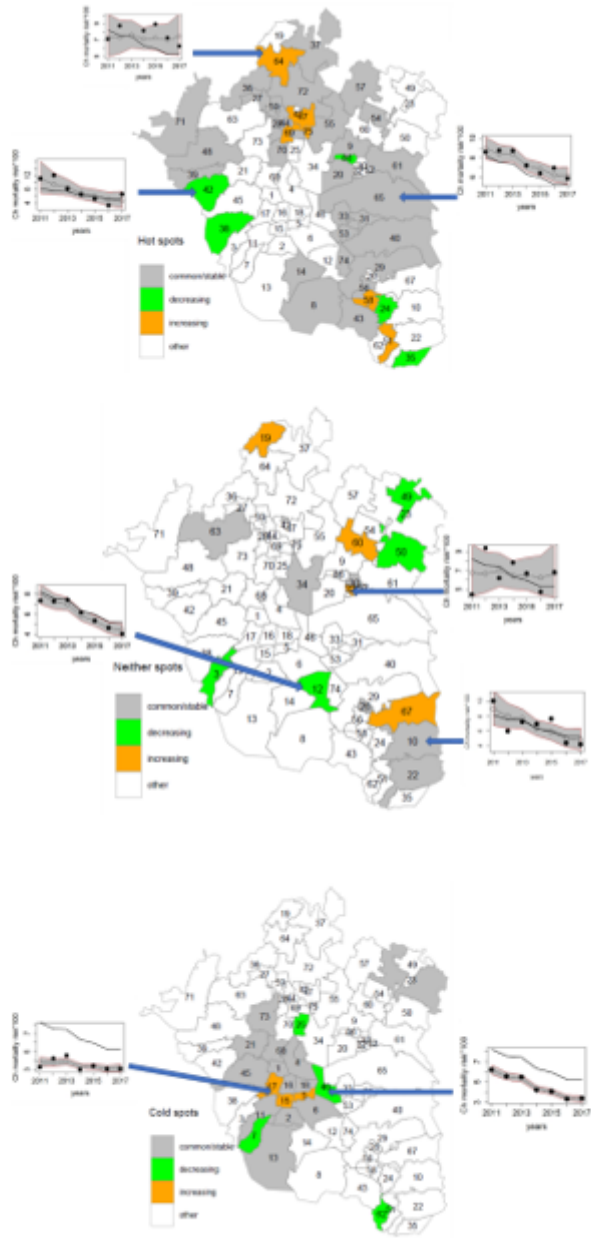


Figure 3

Temporal trends in child mortality risk for high-risk municipalities. Figure 3a displays the temporal dynamics of child mortality risks for high-risk municipalities in Greater Mexico City, which are classified into 3 categories: stable, decreasing and increasing risk. The inserted figures show the observed child mortality risk (black solid dots), the estimated child mortality risks -posterior means of risks- (open circles and dashed line) with a 95% CI (grey region) and the estimated common trend (black line) over time. Temporal trends in child mortality risk for medium-risk municipalities. Figure 3b displays the temporal dynamics of child mortality risk for medium-risk municipalities in Greater Mexico City, which are classified into 3 categories: stable, decreasing and increasing risk. The inserted figures show the

observed child mortality risk (black solid dots), the estimated child mortality risks -posterior means of risks- (open circles and dashed line) with a 95% CI (grey region) and the estimated common trend (black line) over time.TEMPORAL trends in child mortality risk for low-risk municipalitiesFigure 3c displays the temporal dynamics of child mortality risk for low-risk municipalities in Greater Mexico City, which are classified into 3 categories: stable, decreasing and increasing risk. The inserted figures show the observed child mortality risk (black solid dots), the estimated child mortality risks -posterior means of risks- (open circles and dashed line) with a 95% CI (grey region) and the estimated common trend (black line) over time.

Supplementary Files

This is a list of supplementary files associated with this preprint. Click to download.

- [LomeHurtadoetalAppendixamended.pdf](#)